Available online at www.sciencedirect.com
ScienceDirect
Computational Materials Science 39 (2007) 315–323
COMPUTATIONAL MATERIALS SCIENCE
www.elsevier.com/locate/commatsci

Molecular dynamics simulations of the elastic properties of polymer/carbon nanotube composites

Yue Han, James Elliott *

Department of Materials Science and Metallurgy, University of Cambridge, Pembroke Street, Cambridge CB2 3QZ, UK

Received 21 November 2005; received in revised form 14 June 2006; accepted 20 June 2006

Abstract

Carbon nanotubes (CNTs) are promising additives to polymeric materials due to the potential for their enhancement of the structural, mechanical and electronic properties of the resulting composite. However, improvements in properties are by no means guaranteed, and the results are often sensitive to the particular polymer chosen, in addition to the quantity and quality of CNTs used in the composite. In this paper, we present classical molecular dynamics (MD) simulations of model polymer/CNT composites constructed by embedding a single wall (10, 10) CNT into two different amorphous polymer matrices: poly(methyl methacrylate) (PMMA) and poly{(*m*-phenylene-vinylene)-*co*-[(2,5-dioctoxy-*p*-phenylene) vinylene]} (PmPV), respectively, with different volume fractions. A constant-strain energy minimization method was then applied to calculate the axial and transverse elastic moduli of the composite system. The simulation results support the idea that it is possible to use CNTs to mechanically reinforce an appropriate polymer matrix, especially in the longitudinal direction of the nanotube. In addition, the results show that detailed interfacial ordering effects cannot be ignored when interactions between the nanotube and polymer matrix are strong. The comparison of the simulation results with the macroscopic rule-of-mixtures for composite systems showed that for strong interfacial interactions, there can be large deviations of the results from the rule-of-mixtures.

Keywords: Carbon nanotube polymer composites; Molecular dynamics simulations; Energy minimization; Elastic modulus; Interfacial energy

1. Introduction

Carbon nanotubes (CNTs), comprising long, thin cylinders of carbon with multiple wall layers, were first recognized in 1991 by Iijima [1], and later found as single wall entities. Due to their excellent structural, mechanical and electronic properties, CNTs are considered as potentially useful reinforcements for structural and multi-functional composites [2]. One of the first studies of polymer/CNT composites was initially reported by Ajayan et al. [3]. In their research, multi-wall carbon nanotubes (MWNTs) were dispersed randomly in a liquid epoxy resin by mechanical mixing. Since then, many other reports have addressed the fact that incorporating a small percentage of CNTs by weight into polymer matrices could improve mechanical [2,4–7] and electrical [8,9] properties of polymer composites.

It is well established that the performance of a fibre-reinforced composite depends critically on the interfacial characteristics between the fibres and the matrix material. The classical theory of fibre-reinforced composites holds that strong fibre–matrix interfaces lead to high composite stiffness and strength, but also to low composite toughness and *vice versa* [10]. With nanotube-based composites, it may also be the case that strong interfaces would lead to high composite stiffness and strength. There has been much speculation as to whether the strength of the interface between CNTs and polymer matrices is significant at all, and experimental methods for its measurement are rather difficult. Wagner et al. [11] examined the fragmentation of MWNTs in polymer films and estimated that the

* Corresponding author. Tel.: +44 1223 335987; fax: +44 1223 334567.
E-mail address: jae1001@cam.ac.uk (J. Elliott).

0927-0256/$ - see front matter © 2006 Elsevier B.V. All rights reserved.
doi:10.1016/j.commatsci.2006.06.011

MWNT–matrix stress transfer efficiency is at least one order of magnitude larger than that of conventional fibre-based composites. Cooper et al. [12] concluded that the effective modulus of SWNTs dispersed in a composite (epoxy resin/nanotube mixture) could be over 1 TPa and that of MWNTs was about 0.3 TPa. Qian et al. [13] have reported that 1 wt.% CNT additions in a PS matrix result in 36–42% and *ca.* 25% increases in elastic modulus and breaking stress, respectively, indicating significant reinforcement [2,14]. Similar results were also reported by Xu et al. [15] for MWNT/epoxy resin composites. Cadek et al. [16] reported the role of nanotube surface area in the reinforcement of polymer matrices. They suggested that the degree of reinforcement scales linearly with the total nanotube surface area in the films, indicating that small diameter and well dispersed CNTs would give the best results for mechanical reinforcement.

The extent to which mechanical reinforcement can be achieved depends on several factors, including uniformity of dispersion, degree of alignment of CNTs, and the strength of polymer–CNT interfacial bonding. Since it is difficult to control and measure many of these properties experimentally, computational modelling can provide some crucial insights. For this reason, theoretical and computational methods have been widely applied to study polymer/CNT composites. First-principles techniques, molecular mechanics methods and continuum mechanics theories, or combinations thereof, have been attempted for the study of the composite systems. Interfacial strength and stress transfer between CNT and polymers in their composites was studied by Wagner [17] using an expanded form of Kelly–Tyson model and by Lau [18] applying fibre pullout simulations, respectively. Lordi and Yao [19,20] used a molecular mechanics approach to investigate interfacial characteristics of the polymer/CNT composites. In addition to the interfacial behaviour, several groups have also applied computational simulations to calculate the mechanical properties of the polymer/CNT composites [21,22]. The results of their research showed reinforcement after incorporating CNTs into polymer matrix. Despite this, the relation between the elastic properties and the interfacial behaviour still remains poorly understood.

In general, semicrystalline thermoplastic polymers can exhibit relatively large strains compared to other amorphous materials in which only a small elastic strain can be generated before either fracture or yielding takes place. Since the ultimate tensile strength or yield stress are governed by the presence of defects, then the large-scale microstructure of the material is more pertinent than the local atomic structure. Hence it is computationally very difficult to calculate the strength of pure polymer systems, and also in composite systems undergoing large plastic deformations (e.g. fibre pull-out) using the molecular dynamics method. It is for this reason that the current study focuses on the calculation of low strain elastic moduli only, with the principle motivation being an elucidation of the effect of interfacial interaction energy between CNTs and polymer matrices on the elastic moduli of their composites. However, it is certain that these interfacial phenomena will also affect the strength of the composite.

2. Simulation methodology

A standard constant stress molecular dynamics (MD) simulation method was applied to construct the atomistic models of the polymer/CNT composites in this study by setting up an appropriate interatomic potential function (specified in the following discussion). MD simulations are useful to study the time evolution behaviour of systems in a variety of states where thermal sampling of configurational space is required [23]. After equilibration at finite temperature, an energy minimization method was applied to calculate the elastic moduli of the models structures computed from the MD simulations. Periodic boundary conditions were applied to the models along both the tube axis and transverse directions.

2.1. Calculation of the CNT volume fraction

The CNT volume fraction is an important variable in determining the composite mechanical properties. Since the polymer matrix does not penetrate the CNTs, and the (10, 10) SWNT used in the present work had a radius of 1.34 nm, the tube was treated as a solid beam. Therefore its effective volume fraction, f_{CNT}, includes the entire CNT cross-section and is defined by

$$f_{\mathrm{CNT}} = \frac{\pi\left(R_{\mathrm{CNT}} + \frac{h_{\mathrm{vdW}}}{2}\right)^2}{A_{\mathrm{cell}}} \tag{1}$$

where h_{vdW} is the equilibrium van der Waals separation distance between the CNT and the matrix, and A_{cell} is the cross-sectional area of the unit cell transverse to the nanotube axis. The van der Waals separation distance depends on the nature of the CNT–polymer interfacial interactions and was calculated to be 0.18 nm in the present work. A picture of the unit cell of the poly(methyl methacrylate) (PMMA)/CNT composite used in the current study is shown in Fig. 1.

2.2. Calculation of polymer/CNT interaction energy

A strong interfacial interaction between the tube and matrix material is critical to take full advantage of the excellent stiffness and strength of CNTs for reinforcement. In the absence of covalent chemical bonding, the interfacial bond strength comes mainly from the electrostatic and van der Waals forces in the molecular system. The interfacial bond strength between the CNT and polymer can be quantified by the interaction energy, ΔE [21], which is estimated from the energy difference between the total internal energy of the composite and the sum of the energies of individual molecules:

$$\Delta E = E_{\mathrm{total}} - (E_{\mathrm{CNT}} + E_{\mathrm{polymer}}) \tag{2}$$

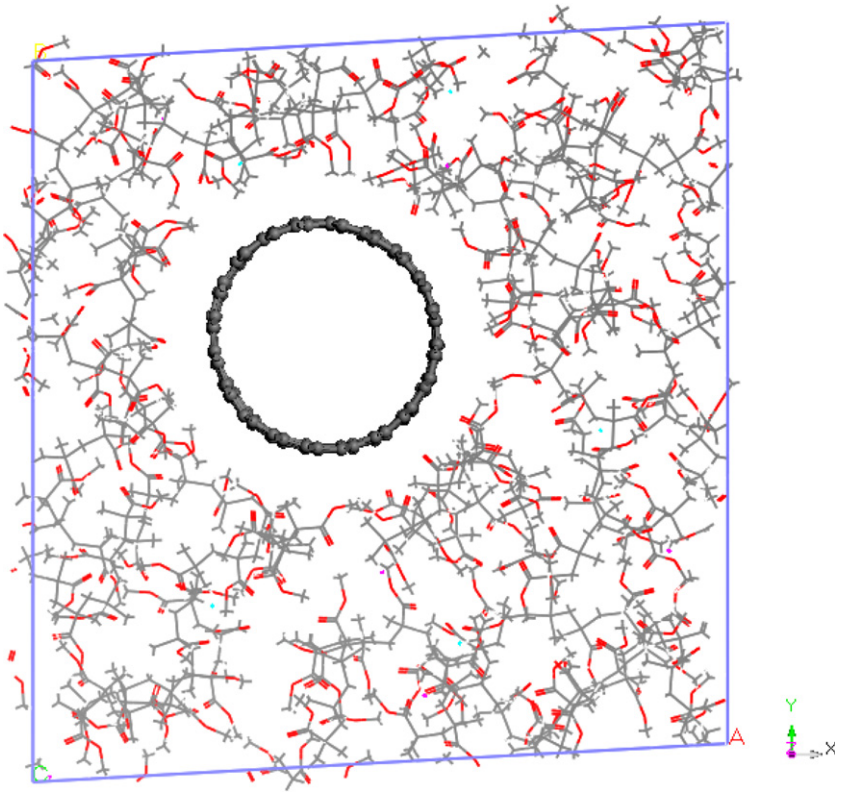

Fig. 1. Snapshot of a MD simulation cell of the PMMA/CNT composite.

where E_{total} is the total internal energy of the polymer/CNT system, E_{CNT} is the energy of the individual CNT and $E_{polymer}$ is the energy of the polymer matrix.

2.3. Building molecular model of the polymer matrix

A description of the method used to build periodic amorphous polymer matrices free from finite size effects and any residual stress is given for PMMA, although a similar method was also used for poly{(*m*-phenylenevinylene)-*co*-[(2,5-dioctoxy-*p*-phenylene)vinylene]} (PmPV) [24]. Two chains of PMMA (80% syndiotactic), each with 50 repeat units, were built in a periodic box with initial density of 0.1 g cm^{-3} using the DREIDING force field parameters [25]. The model was put into an NPT ensemble simulation with a pressure of 10 atm and temperature of 500 K for 1 ns (the simulation time step was 1 fs). The purpose of this step was to slowly compress the structure to generate initial amorphous matrix with the correct density and low residual stresses. Attempts to further increase pressure using the DREIDING force field failed to generate a density close to the experimental value. The COMPASS force field [26] was then applied under the same conditions for another 500 ps. The simulation temperature was then set to 298 K, and pressure of 1 atm for another 500 ps. The density of the final matrix was 1.15 g cm^{-3}, which is very close to the experimental value of 1.19 g cm^{-3}. After this, a constant-strain minimization was carried out with the strain being varied from 0% to 2% in discrete steps, as described in Section 2.4.

2.4. Calculation of the elastic moduli

The constant-strain energy minimization method in Cerius^2 [27] was applied to calculate the elastic moduli of the polymer/CNT composite system. In general, the stress in a solid (or a group of interacting particles in the form of a solid) is defined as the change in the internal energy per unit volume with respect to the strain. Small strains were applied to a periodic structure at an energy minimum. The application of strain was accomplished by uniformly expanding the dimensions of the simulation cell in the direction of the deformation and re-scaling the new coordinates of the atoms to fit within the new dimensions. The structure was then re-minimized keeping the lattice parameters fixed, and the resultant stress in the minimized structure was measured. This was repeated for a series of strains. The variation of the measured stress as a function of applied strain was used to derive the stiffness matrix.

Since the periodic computational cell is triclinic, the system is not isotropic. Thus, the Young's modulus of the PMMA matrix constructed as described in Section 2.3 was calculated by taking the average value in the x, y and z directions. The Young's modulus of a hypothetical isotropic amorphous PMMA matrix from the present simulations is about 2.5 GPa (compared with an experimental

range of between 2.24 and 3.8 GPa). The same process was applied to PmPV, and the Young's modulus calculated was 2.1 GPa.

3. Computational results

3.1. Study of PmPV/CNT composite system

Atomic scale modelling of a polymer/CNT composite system is rather challenging because of the significant number of atoms involved, and equilibration times for the polymer that are orders of magnitude longer than a few nanoseconds, which is typically the limit of large classical molecular dynamics simulations. Thus, the present simulation work is focused on composite systems with a large CNT volume fraction (>10%) in order to reduce the total size of the model. Although experimental systems typically contain much lower volume fractions of CNTs, our simulation results can help to understand interfacial behaviour on an atomic scale, and can make useful predictions for lower CNT volume fraction enhancement by extrapolation.

A (10, 10) SWNT was placed in the centre of a periodic simulation cell. PmPV molecules with different number of repeat units were then placed randomly around the tube in non-overlapping positions. A similar equilibration process as used for generating the matrix model (Section 2.3) was then applied to generate the composite model. The interaction energy between PmPV matrix and CNT was calculated to be about (-360 ± 30) kcal mol^{-1} by the present simulation. The magnitude of the error represents the spread of values of the interaction energy averaged over 10 independently constructed configurations prepared according to the procedure described in Section 2.3, with the negative sign indicating attraction between the PmPV matrix material and the nanotube. The exact nature of these interactions is still unclear in the literature. It is thought that the phenyl ring of the PmPV backbone may attach onto the graphene surface of the carbon nanotube, held via interactions with the sp^2 hybridised atoms of the nanotube. Fig. 2 is a snapshot of a MD simulation model of a (10, 10) SWNT wrapped helically with a single chain PmPV molecule *in vacuo* after equilibration. Our simulations display evidence for strong alignment of the phenyl rings of PmPV parallel to the surface of the graphene sheet, but there is no preferred ordering in the plane of the sheet. Figs. 3 and 4 show the radial distribution functions (RDFs) between carbon atoms in the PmPV/PMMA molecules and the longitudinal axis of the SWNT embedded in the com-

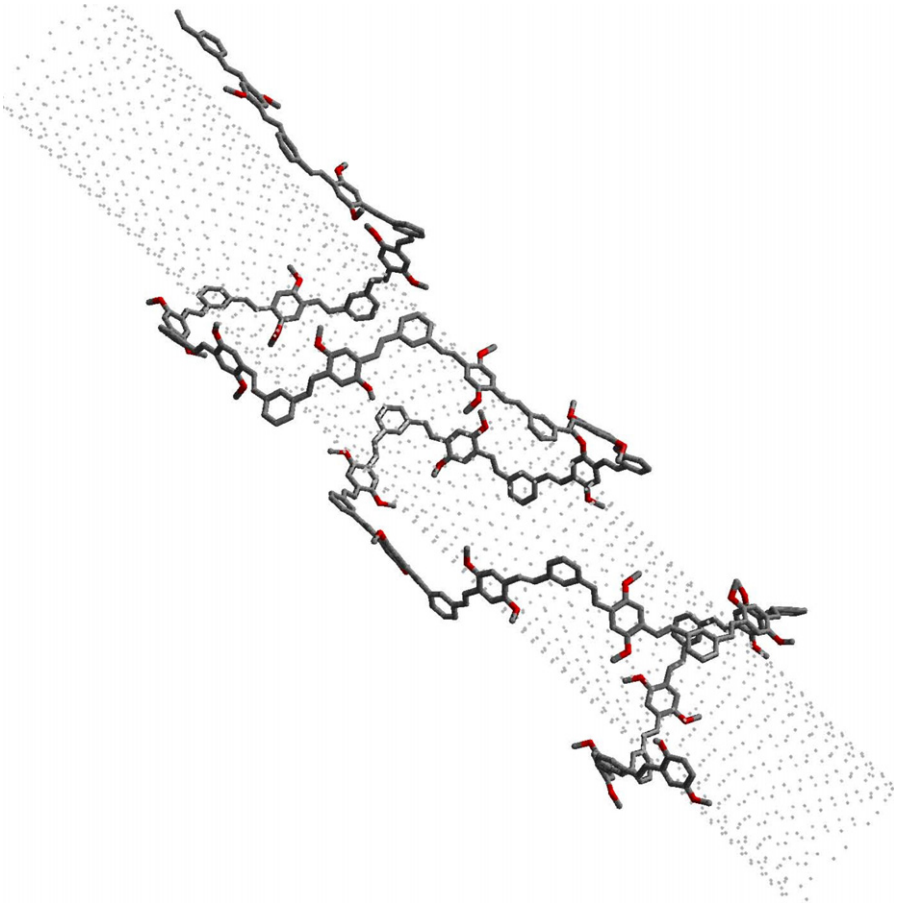

Fig. 2. Snapshot of a MD simulation model of (10, 10) SWNT and PmPV molecule *in vacuo*. Only the backbone of the PmPV molecule is visible in the graph. The SWNT is shown here as small dots.

posite models. It can be seen from Fig. 3 that the aromatic carbon atoms in the backbone of PmPV are closer to the carbon nanotube surface than those carbon atoms in the side chains of PmPV molecule. This further confirms our observation that there is strong alignment of phenyl rings of PmPV parallel to the carbon nanotube surface, which in turn may lead to a higher interaction energy than for the PMMA/CNT composite model, as shown later.

Following equilibration, the amorphous models of PmPV/CNT composites with different CNT volume fractions were then subjected to constant-strain minimization for the calculation of mechanical properties. The stress–strain curves of the composites under transverse and longitudinal loading directions are presented in Figs. 5 and 6, respectively. The legends in the graph represent the CNT volume loading fractions. From the stress–strain curves for different directions, we can see that subjected to transverse loading condition, there is no strong reinforcement of the matrix. This is because the matrix material sustains most of the load in the transverse direction, and also the Young's modulus for SWNTs in the transverse direction (10 GPa in the present calculation) is very small compared with that of the longitudinal direction (600 GPa in the present calculation). However, in the longitudinal direction, the slope of the stress–strain curve (i.e. the Young's modulus) clearly increases with the increasing of CNT volume frac-

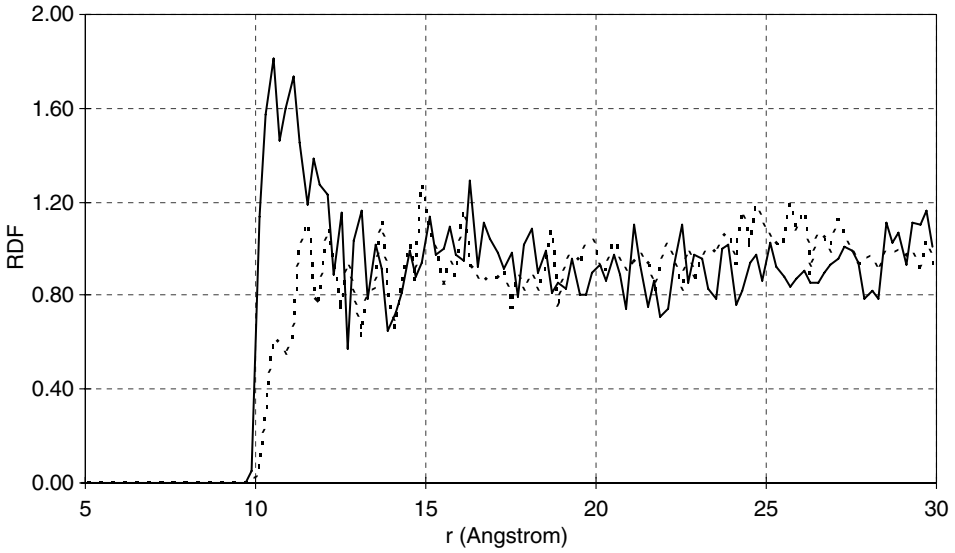

Fig. 3. RDF for the PmPV/CNT composite system. Solid line represents the RDF between carbon atoms of aromatic rings in the backbone of PmPV and the longitudinal axis of the SWNT; dashed line represents the RDF between those carbon atoms in the side chains of PmPV and the longitudinal axis of the SWNT. In both cases, r is the radial distance from the tube axis.

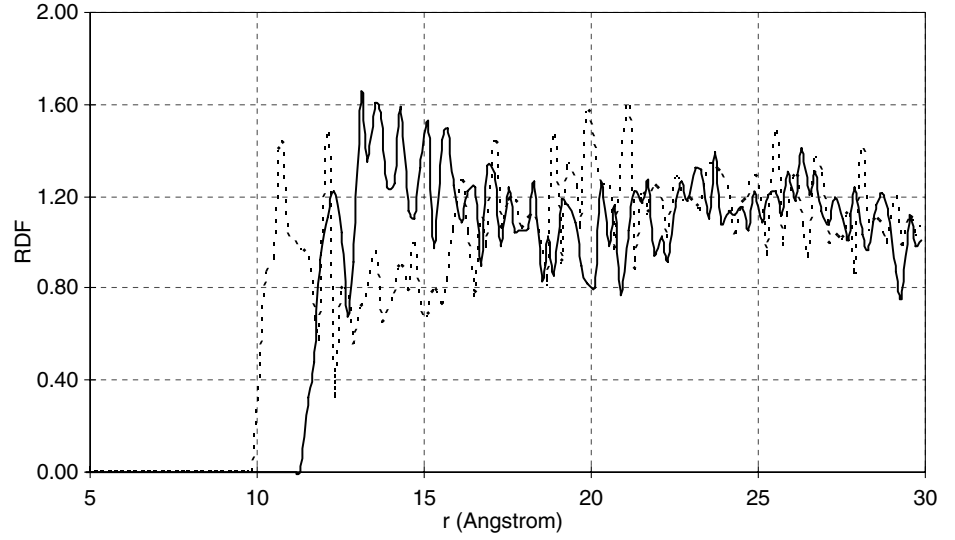

Fig. 4. RDF for the PMMA/CNT composite system. Solid line represents the RDF between carbon atoms in the backbone of PMMA and the longitudinal axis of the SWNT; dashed line represents the RDF between those carbon atoms in the side chains of PMMA and the longitudinal axis of the SWNT. In both cases, r is the radial distance from the tube axis.

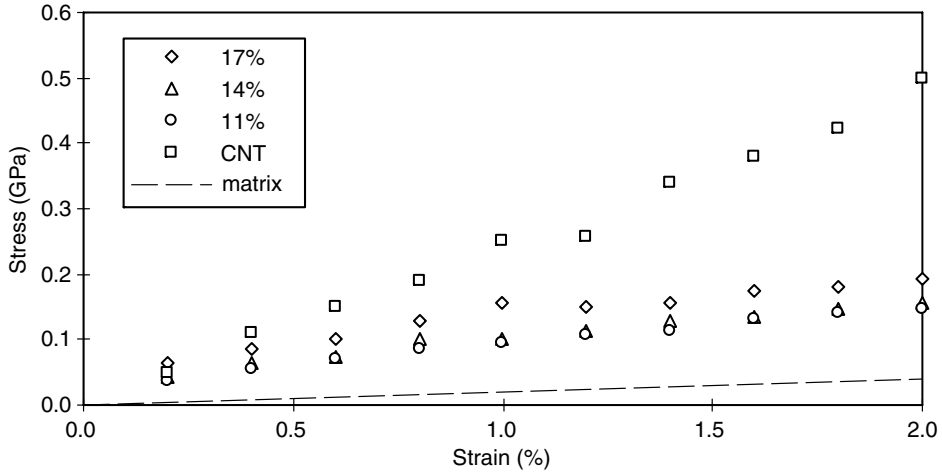

Fig. 5. Stress–strain curves in the transverse direction for PmPV/CNT composites with different CNT volume fractions.

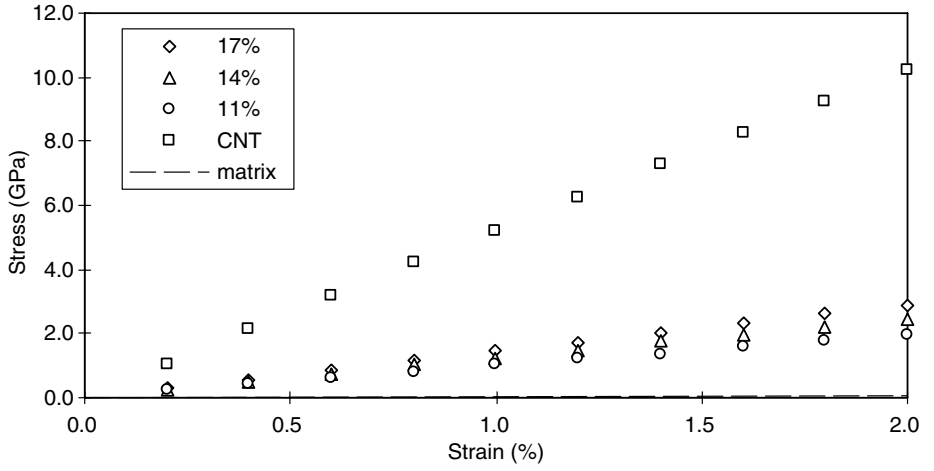

Fig. 6. Stress–strain curves in the longitudinal direction for PmPV/CNT composites with different CNT volume fractions.

tion (CNT have effectively infinite length in the longitudinal direction in the present work), since the CNTs carried most of the load in this direction. Note that for the same strain of 2%, the maximum corresponding stress is about 0.2 GPa in transverse direction, whereas in longitudinal direction, the stress is 2 GPa, which is about ten times larger than the one in the transverse direction.

3.2. Study of PMMA/CNT composite system

A similar process as described in Sections 2.3 and 3.1 was applied to build PMMA/CNT composite system. The interaction energy between PMMA matrix and CNT was calculated to be about (-243 ± 30) kcal mol^{-1} by the present simulation. Again, the magnitude of the error represents the spread of values of the interaction energy averaged over 10 independently constructed configurations prepared according to the procedure described in Section 2.3. It is clear that the magnitude of the interfacial interaction is much smaller than that for the PmPV/CNT system, even allowing for the range of values resulting from averaging over configurations. Both from the RDF graphs (Figs. 3 and 4) and the MD snapshot (Fig. 2), it can be seen that the strong interactions between phenyl rings of PmPV backbone and SWNT surface is a possible reason for the higher interaction energy of the PmPV/CNT system. The longitudinal and transverse stress–strain curves of PMMA/CNT composites generated from constant-strain minimization simulations are presented in Figs. 7 and 8, respectively, with strains varying from 0% to 2%. The difference in longitudinal and transverse behaviour, as shown in Figs. 7 and 8, illustrate the anisotropy of the composite material. Again, it can be seen that the reinforcement behaviour in the longitudinal loading direction is much stronger than that in the transverse direction.

3.3. Comparison of results with conventional rule-of-mixtures

For a composite under uniaxial loading, the elastic modulus can be estimated and predicted by the conven-

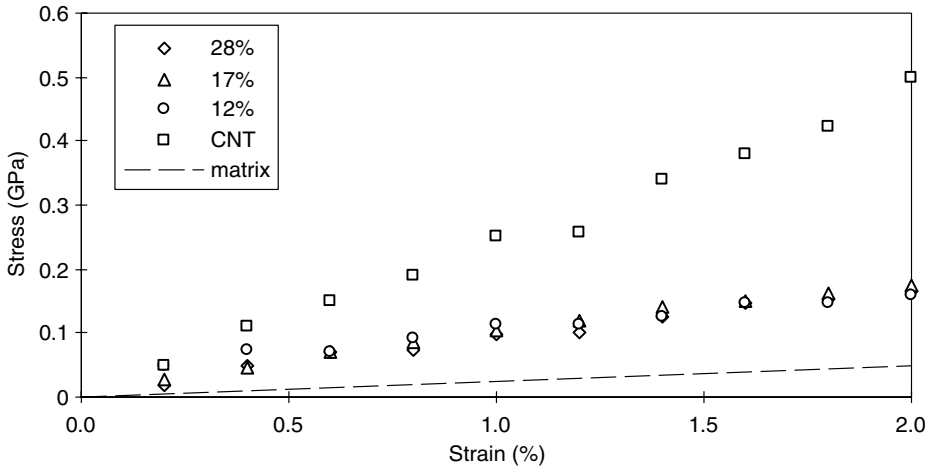

Fig. 7. Stress–strain curves in the transverse direction for PMMA/CNT composites with different CNT volume fractions.

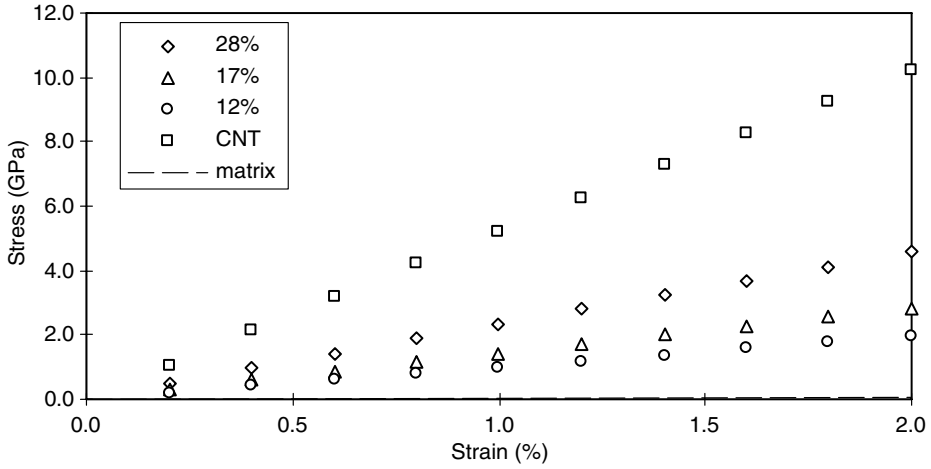

Fig. 8. Stress–strain curves in the longitudinal direction for PMMA/CNT composites with different CNT volume fractions.

tional macroscopic rule-of-mixtures for continuous fibre composites. The rule of mixtures is defined as

$$E_c = \Omega_f E_f + (1 - \Omega_f) E_m \quad (3)$$

where E_c denotes the predicted elastic modulus of the composite, E_f denotes the elastic modulus of the fibre, E_m denotes the elastic modulus of the matrix and Ω_f denotes the volume fraction of the fibre. The results of the comparison between simulation results obtained in the present work and the predictions of Eq. (3) are shown in Fig. 9 (for PMMA) and Fig. 10 (for PmPV), and the numerical results are summarised in Table 1. A longitudinal modulus of 600 GPa and transverse modulus of 10 GPa for (10, 10) SWNT were used here. These modulus values were calculated via constant strain energy minimization method for a hexagonal, infinitely periodic SWNT bundle. The 2D unit cell formed by the centres of adjacent SWNTs in the bundle therefore defined the transverse cross-sectional area per tube. A value of 600 GPa calculated using this method is equivalent to about 1.2 TPa when considering an isolated single wall nanotube modelled as a solid beam. This value is within the range of most of the theoretical and experimental results [28], and the method for the calculation of SWNT bundle modulus is in accordance with that for used the calculation of the polymer/CNT composite modulus.

The last column of Table 1 is calculated by dividing the longitudinal modulus difference between simulation results and the conventional rule of mixtures by the longitudinal modulus of the conventional calculations. The fractional difference represents the deviation of the present simulation results from the conventional rule of mixtures. From both Figs. 9 and 10, and Table 1, it can be seen that the deviation from the conventional rules of the PmPV/CNT composite is larger than that of the PMMA/CNT composite. This could be explained by the interaction energy difference between the two systems. The interaction between matrix and CNT of the PmPV/CNT system, (-360 ± 30) kcal mol^{-1}, is stronger than that of the PMMA/CNT system, (-243 ± 30) kcal mol^{-1}. The results show that the interfacial effects in nanocomposites cannot be ignored when interactions at the interface are strong. The assumption of conventional rule-of-mixtures was that the whole system

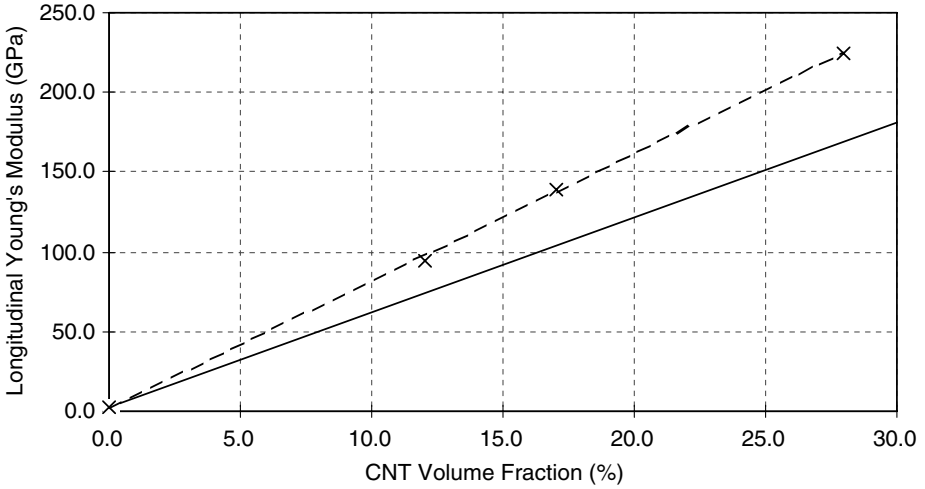

Fig. 9. Comparison of simulation results of PMMA system (dashed line) with conventional rule of mixtures (solid line).

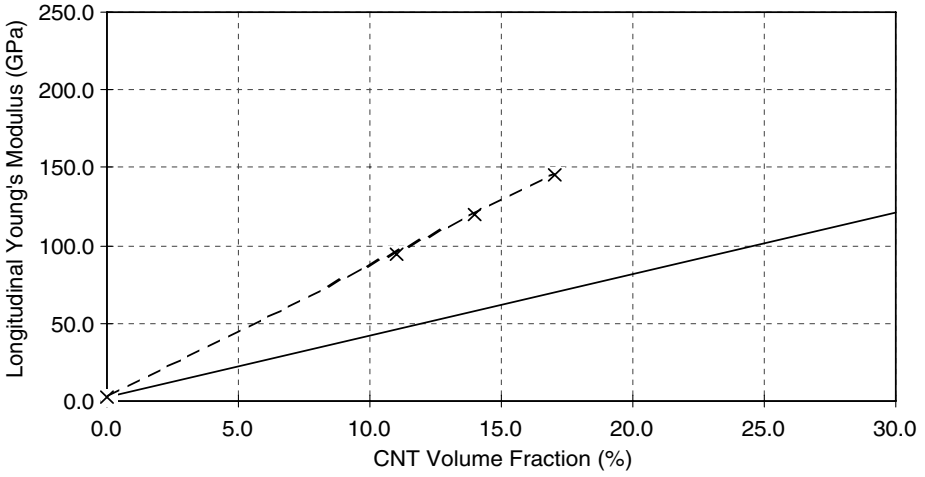

Fig. 10. Comparison of simulation results of PmPV system (dashed line) with conventional rule of mixtures (solid line).

Table 1
Summary of numerical results for elastic modulus of PMMA/PmPV–CNT composite systems

Molecular dynamics results			Rule of mixtures		Fractional difference (longitudinal modulus)
f_{CNT} (%)	T (GPa)	L (GPa)	T (GPa)	L (GPa)	
PMMA/CNT composite					
0.0	2.5	2.5	2.5	2.5	
12.0	2.9	94.6	2.7	71.9	0.32
17.0	4.9	138.9	2.9	105.8	0.31
28.0	5.5	224.2	3.2	171.7	0.31
PmPV/CNT composite					
0.0	2.1	2.1	2.1	2.1	
11.0	2.2	94.8	2.3	67.9	0.40
14.0	2.3	120.2	2.4	85.8	0.40
17.0	3.5	145.6	2.4	103.7	0.40

T represents elastic modulus in transverse direction; L represents modulus in longitudinal direction.

is continuum and that the interfaces between the matrix and filler material remain fully intact. In general, the macroscopic rule-of-mixtures, which takes only the CNT volume fraction into account in determining composite modulus, appears to break down for polymer–CNT composites where there are strong interfacial interactions.

4. Conclusions

Molecular dynamics (MD) and energy minimization simulation methods were employed to investigate the elastic moduli of the polymer/CNT composite systems. Both PMMA and PmPV matrices were studied and compared. The simulation results suggested the possibility of using CNTs to mechanically reinforce both of these two polymer matrices (by increasing the low strain elastic modulus), especially in the tube longitudinal direction. For a fixed tensile load, the CNTs should be aligned parallel with the loading direction to produce the largest tensile modulus. In addition, the results show that interfacial effects cannot be ignored when interactions between the nanotube and polymer matrix are strong. The general macroscopic rule-of-mixtures cannot be applied straightforwardly to composites with strong interfacial interactions. We expect that the stronger the interaction energy between the CNT and the polymer matrix material, the larger the deviation between the simulation results and the rule-of-mixtures.

References

[1] S. Iijima, Nature 354 (56) (1991) 56–58.
[2] E.T. Thostenson, Z. Ren, T.-W. Chou, Composites Science and Technology 61 (2001) 1899–1912.
[3] P.M. Ajayan, O. Stephan, C. Colliex, D. Trauth, Science 256 (5176) (1994) 1212–1214.
[4] S.L. Ruan, P. Gao, X.G. Yang, T.X. Yu, Polymer 44 (19) (2003) 5643–5654.
[5] Y. Ren, F. Li, H.-M. Cheng, K. Liao, Carbon 41 (11) (2003) 2177–2179.
[6] R. Andrews, M.C. Weisenberger, Solid State and Materials Science (2003).
[7] K. Lau, D. Hui, Composites: Part B 33 (2002) 263–277.
[8] K. Yoshino, H. Kajii, H. Arake, T. Sonoda, H. Take, S. Lee, Fullerene Science and Technology 7 (4) (1999) 695–711.
[9] E. Kymakis, I. Alexandou, G.A.J. Amaratunga, Synthetic Metals 127 (1–3) (2002) 59–62.
[10] F.R. Jones, in: D.M. Brewis, D. Briggs (Eds.), Handbook of Polymer–Fiber Composites, Longman Scientific & Technical, Essex, England, 1994.
[11] H.D. Wagner, O. Lourie, Y. Feldman, R. Tenne, Applied Physics Letters 72 (2) (1998) 188–190.
[12] C.A. Cooper, R.J. Young, M. Halsall, Composites: Part A 32 (2001) 401–411.
[13] D. Qian, E.C. Dickey, R. Andrews, T. Rantell, Applied Physics Letters 76 (20) (2000) 2868–2870.
[14] J.H. Gou, B. Minaie, B. Wang, Z.Y. Liang, C. Zhang, Computational Materials Science 31 (3–4) (2004) 225.
[15] X. Xu, M.M. Thwe, C. Shearwood, K. Liao, Applied Physics Letters 81 (15) (2002) 2833–2835.
[16] M. Cadek, J.N. Coleman, K.P. Ryan, V. Nicolosi, G. Bister, A. Fonseca, J.B. Nagy, K. Szostak, F. Beguin, W.J. Blau, Nano Letters 4 (2) (2004) 353–356.
[17] H.D. Wagner, Chemical Physics Letters 361 (2002) 57–61.
[18] K. Lau, Chemical Physics Letters 370 (2003) 399–405.
[19] V. Lordi, N. Yao, Journal of Materials Research 15 (12) (2000) 2770–2779.
[20] K. Liao, S. Li, Applied Physics Letters 79 (2001) 4225–4227.
[21] J. Gou, B. Minaie, B. Wang, Z. Liang, C. Zhang, Computational Materials Science 31 (2004) 225–236.
[22] M. Griebel, J. Hamaekers, Computer Methods in Applied Mechanics and Engineering 193 (2004) 1773–1788.
[23] A.R. Leach, Molecular Modelling: Principles and Applications, second ed., Pearson Education Limited, 2001.
[24] M.i.h. Panhuis, A. Maiti, A.B. Dalton, A.v.d. Noort, J.N. Coleman, B. McCarthy, W.J. Blau, Journal of Physical Chemistry B 107 (2003) 478–482.
[25] S.L. Mayo, B.D. Olafson, W.A. Goddard, Journal of Physical Chemistry 94 (1990) 8897–8909.
[26] H. Sun, Journal of Physical Chemistry B 102 (1998) 7338–7364.
[27] Cerius^2 User Guide, Molecular Simulation Inc., San Diego, 1997.
[28] K.T. Lau, M. Chipara, H.Y. Ling, D. Hui, Composites Part B: Engineering 35 (2) (2004) 95–101.